PHYSICAL REVIEW A **89**, 030501(R) (2014)

# Photoreactions with universal trimers

Betzalel Bazak* and Nir Barnea†
*Racah Institute of Physics, The Hebrew University, 91904, Jerusalem, Israel*
(Received 19 May 2013; revised manuscript received 30 October 2013; published 21 March 2014)

Considering one-body and two-body currents, we study the photoassociation and photodissociation of universal bosonic trimers. Analyzing the relative importance of these currents, we identify two physical scenarios: (i) normal hierarchy, where naive power counting holds and the one-body current dominates, and (ii) strong hierarchy, where the one-body current is suppressed. For both scenarios we observe that at the high-frequency tail, the response function exhibits log-periodic oscillations in transition to or from any continuum state regardless of the reaction partial-wave channel. In contrast, near-threshold log-periodic oscillations appear only in the leading $s$-wave components. These oscillations are the fingerprints of universal Efimov physics. We discuss the relevance of this effect to contemporary experiments in ultracold atoms.

DOI: 10.1103/PhysRevA.89.030501 PACS number(s): 31.15.ac, 67.85.−d, 34.50.−s

*Introduction*. The low-energy physics of two neutral particles interacting via a short-range force depends on a single parameter, the $s$-wave scattering length $a$. As long as the energy of the system is much smaller than $\hbar^2/Mr_0^2$, the energy scale associated with the typical range of the potential $r_0$ and the mass $M$, the properties of the system are indifferent to the details of the interparticle force. In this limit the system is said to exhibit universal behavior that is independent of its actual constituents.

The window for probing universality opens up when the scattering length $a$ is much larger than the typical range of the potential $r_0$. Such is the situation in nuclear physics [1], in helium molecules [2], and in magnetically manipulated ultracold atoms [3].

Under the condition $|a| \gg r_0$, universality can be manifested not only in the two-body case but also in other few- and many-body systems. The system of three identical bosons is a particular case. In the limit of a resonating two-body interaction $|a| \to \infty$, universality is associated with a series of weakly bound three-body states, known as Efimov trimers [4,5], that appear even when the interaction supports no bound dimer. The spectra of these trimers reveal a discrete scaling symmetry, resulting from quantum mechanical breaking of classical scaling symmetry, that also yields log-periodic oscillations in the trimer's wave function.

These log-periodic oscillations are the fingerprints of the Efimov effect. They were predicted to appear in various aspects of universal trimer physics. One example is the oscillations of the three-body recombination rate constant as a function of the scattering length $a$ [6–11]. Other examples revealing log-periodic oscillations are the atom-dimer scattering length [12] and disintegration cross section, and the energy-dependent collisional recombination rate of Efimov trimers in cold gas [13].

In this Rapid Communication we discuss another aspect of the Efimov effect that has drawn very little attention so far, that is, the appearance of log-periodic oscillations in the photoreaction cross section of universal trimers. To this end we consider one-body and two-body currents and analyze their relative importance.

*Photoreactions*. The photodissociation and the photoassociation cross sections are both related through kinematic factors to the photoresponse function

$$S(\omega) = \bar{\sum_i} \sum_f |\langle \Psi_f | \hat{H}_I | \Psi_B, \boldsymbol{k}\lambda \rangle|^2 \delta(E_f - E_B - \hbar\omega) \quad (1)$$

that describes the transition of the trimer from a bound state $\Psi_B$ with binding energy $E_B$ into a continuum state $\Psi_f$ with energy $E_f$ by absorbing a photon of momentum $\boldsymbol{k}$, polarization $\lambda$, and energy $\hbar\omega = \hbar kc$. $\sum_f$ stands for integration over the final states and $\bar{\sum_i}$ averages over the appropriate initial states.

The coupling between neutral particles and the radiation field takes the form $\hat{H}_I = -e \int d\boldsymbol{x} \boldsymbol{\mu}(\boldsymbol{x}) \cdot \nabla \times \boldsymbol{A}(\boldsymbol{x})$, where $\boldsymbol{\mu}$ is the magnetization density and $\boldsymbol{A}$ is the electromagnetic field. In effective low-energy theory [14] the magnetization density contains not only one-body current, but also two-body and more body currents,

$$\boldsymbol{\mu}(\boldsymbol{x}) = \boldsymbol{\mu}^{(1)}(\boldsymbol{x}) + \boldsymbol{\mu}^{(2)}(\boldsymbol{x}) + \cdots . \quad (2)$$

Using low-momentum expansion, the operators in the theory can be arranged in powers of $k/\Lambda$ and $Q/\Lambda$, where $Q$ is the typical particle momentum of the system under consideration. $\Lambda$ is the cutoff momentum of the theory, reflecting the point $\sim\hbar/r_0$ at which short-range physics, ignored by the low-energy theory, is becoming important. At the leading order (LO) and next to leading order (NLO) the one-body current takes the form [15]

$$\boldsymbol{\mu}^{(1)}(\boldsymbol{x}) = \sum_j \boldsymbol{s}_j \left( \mu_0 + L_1 \frac{\boldsymbol{k}^2}{\Lambda^2} \right) \delta(\boldsymbol{x} - \boldsymbol{r}_j), \quad (3)$$

where $\mu_0$ is the magnetic moment of a single particle, $\boldsymbol{r}_j, \boldsymbol{s}_j$ are the position and spin of particle $j$, and $L_1$ is a shape parameter describing the particle's form factor. The two-body contribution to the current enters at the next order ($\mathrm{N^2LO}$), or $(Q/\Lambda)^3$, and takes the form [15]

$$\boldsymbol{\mu}^{(2)}(\boldsymbol{x}) = \sum_{i<j} (\boldsymbol{s}_i + \boldsymbol{s}_j) \frac{L_2}{\Lambda^3} \delta\left( \boldsymbol{x} - \frac{\boldsymbol{r}_i + \boldsymbol{r}_j}{2} \right) \delta_\Lambda(\boldsymbol{r}_i - \boldsymbol{r}_j). \quad (4)$$

*betzalel.bazak@mail.huji.ac.il
†nir@phys.huji.ac.il

 

The low-energy parameter $L_2$ is the coupling constant between the radiation field and the four boson fields. Its value can be fixed studying dimer photoreactions. The notation $\delta_\Lambda(\boldsymbol{r})$ stands for Dirac's $\delta$ function smeared over distance $\hbar/\Lambda$.

Three-body currents, associated with two more bosonic fields, are suppressed by another factor of $(Q/\Lambda)^3$ relative to the N$^2$LO two-body current. Consequently, in the low-energy limit $Q \ll \Lambda$ they can be ignored.

For the bosonic system we assume that the initial- and final-state wave functions can be written as a product of a symmetric spin $|\chi\rangle$ and configuration space $|\psi\rangle$ components, $|\Psi\rangle = |\psi\ \chi\rangle$. We shall further assume that the spin component of the wave function is frozen throughout the photoreaction process, thus $|\chi_f\rangle = |\chi_B\rangle$. Using these assumptions, the one-body transition matrix element in (1) takes the form

$$\langle\Psi_f|\hat{H}_I^{(1b)}|\Psi_B,\boldsymbol{k}\lambda\rangle = -i\sqrt{\frac{\hbar c^2}{2V\omega_k}}\left(\mu_0 + L_1\frac{\boldsymbol{k}^2}{\Lambda^2}\right)\langle\boldsymbol{s}\rangle\sum_{j=1}^{3}\langle\psi_f|e^{i\boldsymbol{k}\cdot\boldsymbol{r}_j}|\psi_B\rangle, \quad (5)$$

whereas the two-body reads

$$\langle\Psi_f|\hat{H}_I^{(2b)}|\Psi_B,\boldsymbol{k}\lambda\rangle = -i\sqrt{\frac{\hbar c^2}{2V\omega_k}}\frac{L_2}{\Lambda^3}2\langle\boldsymbol{s}\rangle\sum_{i<j}^{3}\langle\psi_f|e^{i\boldsymbol{k}\cdot(\boldsymbol{r}_i+\boldsymbol{r}_j)/2}\delta_\Lambda(\boldsymbol{r}_i-\boldsymbol{r}_j)|\psi_B\rangle. \quad (6)$$

Here $\langle\boldsymbol{s}\rangle = \frac{1}{3}\sum_j\langle\chi_B|\boldsymbol{s}_j\cdot(\boldsymbol{k}\times\hat{e}_{\boldsymbol{k}\lambda})|\chi_B\rangle$, and we have used box normalization of volume $V$.

The appearance of log-periodic oscillations in the high-frequency tail of spin-flip rf reactions in ultracold atoms was recently predicted by Braaten *et al.* [16]. Studying rf reactions in the unitary limit $a \to \infty$, they used effective-field theory methods to analyze the Franck-Condon factor dominating photoinduced spin-flip reactions and found that, in the limit $\omega \to \infty$, the three-body response function takes the form $\{A_1 + A_2\sin[s_0\ln(\hbar\omega/|E_B|) + 2\phi]\}/(2m\omega^2)$, where $A_1, A_2, \phi$ are constants, and $s_0 \approx 1.006\,24$ is the Efimov parameter.

For frozen-spin reactions the Franck-Condon term is zero, nonetheless, under the assumptions leading to Eqs. (5) and (6), we will show in the following that (i) in the unitary limit, the high-frequency tail of the response function contains log-periodic oscillations in all partial waves and (ii) the leading $s$-wave component of the response function exhibits log-periodic oscillations throughout the spectrum, from threshold to infinity.

In the long-wavelength limit, the exponent in the LO one-body matrix element, Eq. (5), can be expanded to yield

$$\sum_{j=1}^{3}e^{i\boldsymbol{k}\cdot\boldsymbol{r}_j} \approx 3 + i\sum_{j=1}^{3}\boldsymbol{k}\cdot\boldsymbol{r}_j - \frac{1}{6}\sum_{j=1}^{3}k^2r_j^2 - \frac{4\pi}{15}\sum_{j=1}^{3}k^2r_j^2\sum_m Y_{2-m}(\hat{k})Y_{2m}(\hat{r}_j) + \cdots, \quad (7)$$

where $Y_{lm}$ are the spherical harmonics. The zeroth-order operator is just the Franck-Condon factor which dominates the spin-flip reaction [17], but has no contribution in frozen-spin reactions. The first-order operator is the dipole, which for identical particles is proportional to the center of mass and hence does not affect the relative motion of the particles. Consequently, the one-body current is dominated by the $O((kr)^2)$ quadrupole and $r^2$ operators [18,19].

Assuming that the photon energy is of the order of the binding energy $E_B$ and observing that $r \approx \sqrt{\hbar^2/ME_B}$, the long-wavelength expansion parameter can be written as $kr \approx \sqrt{E_B/Mc^2} \approx Q/Mc$. Comparing $Q/Mc$ to the low-energy expansion parameter $Q/\Lambda$, we see that the importance of the two-body current depends on the relative magnitude of the two high-momentum scales $\Lambda$ and $Mc$. If the scales are such that $Q/\Lambda \ll \Lambda/Mc$, the two-body currents appearing at order $(Q/\Lambda)^3$ are expected to be much smaller than the second-order $(kr)^2 \approx (Q/Mc)^2$ terms. Under these circumstances, we have *normal hierarchy*, as suggested by naive power counting. This is the situation in any effective low-energy theory in the limit $Q \to 0$. The electromagnetic currents in nuclear physics are a fine example of this hierarchy (see, e.g., Refs. [15,20,21]). On the other hand, when the short-range energy scale is much smaller than the mass scale $\Lambda \lll Mc$, we can face a situation where the one-body current proportional to $(Q/Mc)^2$ becomes negligible in comparison to the two-body current. This case of *strong hierarchy* is typical for frozen-spin experiments in ultracold atoms [22–24]. There, the ratio between the scattering length and the effective range is much smaller than the separation between the mass scale and the binding energy.

In the following, after addressing the three-body wave function in the unitary limit, we will analyze these two limiting physical scenarios of normal and strong hierarchies.

*The three-body system.* The dynamics of a quantum three-particle system is governed by the Hamiltonian $H = T + U$, where $T$ is the kinetic energy operator and the potential $U$ is a sum of two- and three-body forces. Removing the center-of-mass coordinate, the system can be described by the Jacobi vectors $\boldsymbol{x} = \sqrt{\frac{1}{2}}(\boldsymbol{r}_2 - \boldsymbol{r}_1)$ and $\boldsymbol{y} = \sqrt{\frac{2}{3}}(\boldsymbol{r}_3 - \frac{\boldsymbol{r}_1+\boldsymbol{r}_2}{2})$, which we transform into the hyperspherical coordinates $(\rho,\Omega)$. $\rho^2 = x^2 + y^2$, $\Omega = (\alpha,\hat{x},\hat{y})$, and $\tan\alpha = x/y$.

For low-energy physics, when the extension of the wave function is much larger than the range of the two-body potential, one can utilize the zero-range approximation, where the action of the potential is represented through appropriate boundary conditions when two particles approach each other [25]. In a similar fashion, the short-range three-body force can be replaced by the boundary condition $\partial\log\psi/\partial\log\rho = C$ at $\rho = \rho_0$. Here we shall assume a hard-core potential, i.e., $C \to \infty$. The cutoff hyperradius $\rho_0$ is our three-body parameter, and it can be fitted, for example, to the trimer's binding energy.

A remarkable aspect of the zero-range approximation in the unitary limit is the factorization of the wave function into a product of hyperangular and hyperradial terms [26], $\psi(\rho,\Omega) = \rho^{-5/2}\mathcal{R}(\rho)\Phi_\nu(\Omega)$. The hyperangular channel functions $\Phi_\nu(\Omega)$ are the solutions of the adiabatic hyperangular equation with eigenvalue $\nu^2$. The hyperradial functions $\mathcal{R}(\rho)$ are the solutions of the hyperradial equation

$$\left(-\frac{\partial^2}{\partial\rho^2} + \frac{\nu^2 - 1/4}{\rho^2}\right)\mathcal{R}(\rho) = \epsilon\mathcal{R}(\rho), \quad (8)$$

subject to the boundary condition $\mathcal{R}(\rho_0)=0$. Here $\epsilon = 2ME/\hbar^2$. The lowest eigenvalue of the adiabatic hyperangular equation appears in the $s$-wave channel $\nu_0 = is_0$, and all other eigenvalues are positive. The Efimov effect [4] results from the fact that $\nu_0$ is imaginary. It is limited to the $s$ wave as there are no imaginary eigenvalues of the hyperangular equation in any other channel.

Substituting $\mathcal{R} = \sqrt{\rho}u(\rho)$, the hyperradial equation is just the Bessel equation. The bound-state solution for the lowest channel is proportional to the modified Bessel function of the second kind and imaginary order, $\sqrt{\rho}K_{is_0}(\kappa\rho)$, where $\kappa = \sqrt{-\epsilon}$. The value of $\kappa$ is fixed by the three-body boundary condition at $\rho_0$. The result is the discrete Efimov spectrum, $\epsilon_n/\epsilon_0 = e^{-2\pi n/s_0} \approx 515^{-n}$. The normalized wave functions are

$$\mathcal{R}_B^{(n)}(\rho) = N_B\kappa_n\sqrt{\rho}K_{is_0}(\kappa_n\rho), \tag{9}$$

where $N_B = \sqrt{2\sinh(s_0\pi)/s_0\pi}$.

For scattering states $\epsilon > 0$ the hyperradial wave function is composed of the Bessel functions of the first and second kind of order $\nu$, and the real part of these functions if $\nu$ is imaginary,

$$\mathcal{R}_f(\rho) = \sqrt{\frac{q\rho N_s}{R}}\{\sin\delta\,\mathrm{Re}[J_\nu(q\rho)] + \cos\delta\,\mathrm{Re}[Y_\nu(q\rho)]\}, \tag{10}$$

where $q=\sqrt{\epsilon}$. Here we assume normalization in a sphere of radius $R$, and $N_s = 1/2\ (\pi)$ for imaginary (real) $\nu$. The phase shift $\delta$ is to be found from the boundary condition $\mathcal{R}_f(\rho_0)=0$.

*Normal hierarchy*. For the normal hierarchy case, the one-body current dominates the photoreaction and the transition matrix element is given by (5). It can be written as a power series in the hyperradius $\rho$ in the following form, $\beta_1\sum_j e^{i\boldsymbol{k}\cdot\boldsymbol{r}_j} = \sum_{m=0,\mu}^{\infty}\mathcal{A}_{m\mu}\rho^m\mathcal{Y}_\mu(\Omega)$, where $\beta_1$ is a prefactor that can be deduced from (5), $\mathcal{Y}_\mu(\Omega)$ are the hyperspherical harmonics [27] that span the hypersphere $\Omega$, and $\mathcal{A}_{m\mu}$ are the expansion coefficients. Substituting this expansion into (5), the transition matrix element between a bound $s$-wave state and a continuum state is

$$\langle\psi_f|\beta_1\sum_j e^{i\boldsymbol{k}\cdot\boldsymbol{r}_j}|\psi_B\rangle = \sum_{m\mu}\mathcal{A}_{m\mu}C^{\mu}_{\nu\nu_0}\int d\rho\mathcal{R}_f^*\rho^m\mathcal{R}_B, \tag{11}$$

where $C^{\mu}_{\nu\nu_0} = \langle\Phi_\nu|\mathcal{Y}_\mu|\Phi_{\nu_0}\rangle$ are the hyperangular matrix elements. Here and in the following we omit the trimer's excitation index $n$ since the discussion applies to any of these states.

Substituting Eqs. (9) and (10), the matrix elements are proportional to integrals of the type

$$\mathcal{I}_J(\nu,m) = \int_{\rho_0}^{\infty} d\rho\,\mathrm{Re}[J_\nu(q\rho)]\rho^{m+1}K_{is_0}(\kappa\rho) \tag{12}$$

or $\mathcal{I}_Y(\nu,m)$, with $Y_\nu$ replacing $J_\nu$. We note that the bound state is invariant to the Efimov scaling $\rho_0 \to e^{-\pi/s_0}\rho_0$, therefore we can replace the lower limit of the integral by zero [28]. Evaluating the integral we get

$$\mathcal{I}_J(\nu,m) = \mathrm{Re}\left[\frac{2^m N^m_{\nu_0,\nu}}{\kappa^{m+2}}\left(\frac{q}{\kappa}\right)^{\nu}{}_2F_1(a,b;c;-(q/\kappa)^2)\right], \tag{13}$$

where ${}_2F_1$ is the hypergeometric function with parameters $a=\frac{m-\nu_0+\nu}{2}+1$, $b=\frac{m+\nu_0+\nu}{2}+1$, and $c=\nu+1$, and $N^m_{\nu_0,\nu} = \Gamma(a)\Gamma(b)/\Gamma(c)$. Similar results are obtained for $\mathcal{I}_Y$.

In the limit of reaction close to threshold, $q \ll \kappa$, this expression can be approximated by

$$\mathcal{I}_J(\nu,m) \approx \mathrm{Re}\left[\frac{2^m N^m_{\nu_0,\nu}}{\kappa^{m+2}}\left(\frac{q}{\kappa}\right)^{\nu}\right]. \tag{14}$$

For an $s$-wave transition the particles in the final state may move along the $\nu=\nu_0$ adiabatic potential, and since $(q/\kappa)^{\nu_0} = \cos(s_0\ln\frac{q}{\kappa}) + i\sin(s_0\ln\frac{q}{\kappa})$, the response function acquires log-periodic oscillations. The remarkable aspect of this result is the fact that, in the long-wavelength limit, the $s$-wave transition operator $r^2$ is the dominant multipole, and therefore they can be observed, in principle, studying photoreactions of Efimov trimers close to threshold.

In the limit of large energy transfer where $q \gg \kappa$, but still smaller than the cutoff momentum $\Lambda$, the reaction probes the short-range part of the trimer's wave function and the transition integral takes the form

$$\mathcal{I}_J(\nu,m) \approx \frac{2^{m+1}}{q^{m+2}}\mathrm{Re}\left[\frac{\Gamma(\nu_0)\Gamma\left(\frac{m-\nu_0+\nu}{2}+1\right)}{\Gamma\left(\frac{-m+\nu_0+\nu}{2}\right)}\left(\frac{q}{\kappa}\right)^{\nu_0}\right]. \tag{15}$$

This result indicates that for any $\nu$ the transition matrix element exhibits log-periodic oscillations in the large energy tail, attenuated by $q^{-m-2}$. These oscillations reflect the structure of the Efimov trimers at short distances, Eq. (9). Consequently, the number of oscillations will reflect the number of nodes in the trimer's wave function.

At this point we would like to study in some detail the response function associated with the $r^2$ operator. As we have already indicated, for normal hierarchy this is the dominant term at low photon energies [29]. The $r^2$ operator is extremely simple, $\sum_j r_j^2 = \rho^2 + 3R^2_{\mathrm{c.m.}}$, where $R_{\mathrm{c.m.}}$ is the center-of-mass radius, and therefore

$$\langle\psi_f| - \frac{\beta_1}{6}\sum_j k^2 r_j^2|\psi_B\rangle = -\frac{\beta_1 k^2}{6}N_B\kappa\sqrt{\frac{qN_s}{R}}\mathcal{I}(\nu_0,2), \tag{16}$$

where $\mathcal{I}(\nu_0,m) = \mathcal{I}_J(\nu_0,m)\sin\delta + \mathcal{I}_Y(\nu_0,m)\cos\delta$ is the sum of the $J$ and $Y$ transition matrix elements $\mathcal{I}_J,\mathcal{I}_Y$ with $m=2$.

To better understand our results, we evaluate the asymptotic expressions for the reaction matrix elements at threshold and at the high-energy tail. In the limit of $q \ll \kappa$ we obtain

$$\mathcal{I}_J(\nu_0,2) \approx \frac{B_1}{\kappa^4}\cos\left(s_0\ln\frac{q}{\kappa}+\phi\right), \tag{17}$$

where $B_1 = 4|\nu_0+1| \approx 5.6745$, $\phi = \tan^{-1}s_0 \approx 0.788\,51$. The phase shift is also a log-periodic function, consequently, near the threshold, the matrix element can be well approximated by

$$\mathcal{I}(\nu_0,2) \approx 1 + \frac{B_2}{2}\cos\left(2s_0\ln\frac{q}{\kappa}\right), \tag{18}$$

where $B_2 \approx 8.475\%$ is the normalized amplitude of these oscillations.

Similarly, in the limit $q \gg \kappa$, one gets

$$\mathcal{I}_J(\nu_0,2) \approx -\frac{B_1}{q^4}\sin\left(s_0\ln\frac{q}{\kappa}+\phi\right). \tag{19}$$

However, in this limit, $\delta \approx \pi/4 - q\rho_0$, and the log-periodic oscillations are masked by these linear oscillations. This

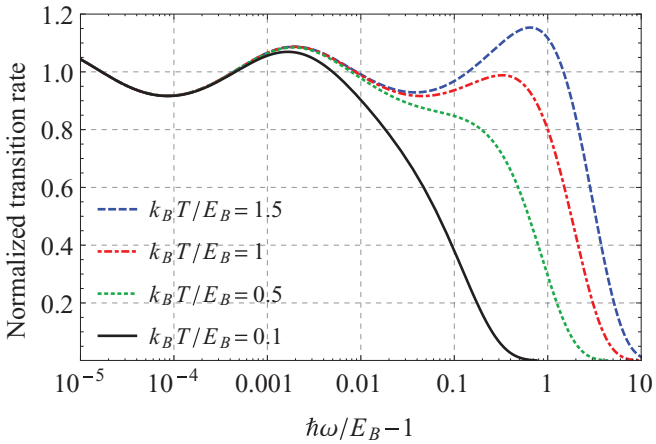


FIG. 1. (Color online) Normalized trimer photoassociation rate as a function of rf photon frequency for different gas temperatures. Blue dashed line: $k_BT = 1.5E_B$; red dotted-dashed line: $k_BT = E_B$; green dotted line: $k_BT = 0.5E_B$; and black line: $k_BT = 0.1E_B$.

situation will certainly complicate an experimental attempt to probe the log-periodic oscillations in this limit.

Substituting the results (16)–(19) in (1), we get a closed-form expression for the response function. Utilizing this response function, the trimer photoassociation rate in a gas of temperature $T$ can be easily calculated by averaging the response weighted with the probability $P(q)$ of finding three particles in the appropriate continuum state. Assuming the system is in thermal equilibrium with temperature $T$, higher than the condensation temperature, $P(q) = \frac{1}{\mathcal{Z}}\frac{R}{\pi}e^{-\beta\hbar^2q^2/2M}$ [29]. In Fig. 1 we present the resulting transition rates for gas with temperatures $k_BT = 1.5E_B$, $k_BT = E_B$, $k_BT = 0.5E_B$, and $k_BT = 0.1E_B$. It can be seen that the number of visible peaks in the trimer photoassociation rate depends on the gas temperature, as the oscillations are suppressed for $\hbar\omega \gtrsim k_BT$ by the Boltzmann factor. In the scale presented here the log-periodic oscillations at the high-frequency tail are unobservable. In reality, the lifetime of the trimer may be short and the oscillations at energies smaller than the trimer energy width may be smeared.

*Strong hierarchy*. In the case of strong hierarchy where $\Lambda \lll M$ and $(Q/\Lambda)^3 \gg (Q/M)^2$, the subleading two-body current becomes dominant and the LO one-body current is suppressed and becomes negligible. The transition matrix element (1) is then dominated by the leading two-body term (6) $\beta_2\langle\psi_f|\sum_{i<j}\delta_\Lambda(\boldsymbol{r}_i - \boldsymbol{r}_j)|\psi_B\rangle = 3\beta_2/\sqrt{8}\langle\psi_f|\delta_\Lambda(\boldsymbol{x})|\psi_B\rangle$, with $\beta_2 = -i\sqrt{\frac{\hbar c^2}{2V\omega_k}}\frac{L_2}{\Lambda^3}2\langle\boldsymbol{s}\rangle$.

The behavior of the wave function when two particles approach each other is governed by the contact interaction. In particular, in the limit $x \to 0$, $\psi \approx \rho^{-5/3}\mathcal{R}(\rho)[\sin(\frac{\pi\nu_0}{2})/2\alpha + O(1) + O(\alpha) + \cdots]$. Utilizing this result we get

$$\langle\Psi_f|H_I|\Psi_B,\boldsymbol{k}\lambda\rangle = \int_0^\infty d\rho\frac{1}{\rho}\mathcal{R}_f^*(\rho)\mathcal{R}_B(\rho)[A\Lambda^2|\sin(\pi\nu_0/2)|^2 + O(\Lambda) + O(1) + \cdots], \quad (20)$$

At an interparticle distance $r \approx \hbar/\Lambda$, the zero-range approximation breaks down. Nevertheless, the details of the wave function at distance $r \leqslant \hbar/\Lambda$, as well as the details of the regulator, i.e., the exact form of $\delta_\Lambda(\boldsymbol{x})$, do not affect the structure of the solution.

The hyperradial integral in (20) is nothing but $\mathcal{I}(\nu_0, -1) = \mathcal{I}_J(\nu_0, -1)\sin\delta + \mathcal{I}_Y(\nu_0, -1)\cos\delta$ given by (13). Comparing this result with Eq. (16), we conclude that near threshold $q \ll \kappa$ the behavior of the photoreaction cross section is the same for both the strong and the normal hierarchy cases.

Considering now higher partial waves, we can utilize the completeness of the hyperspherical harmonics and expand the exponent in (6) into a power series in $\rho$ and hyperspherical harmonics, following the same arguments leading to Eq. (11). The resulting transition matrix elements are again proportional to the $\mathcal{I}_J$,$\mathcal{I}_Y$ integrals (12). Consequently, log-periodic oscillations will appear in the high-energy tail of the cross section, in the same manner as in the normal hierarchy case.

*Summary*. We have explored photoreactions in universal Efimov trimers. We analyzed two physical scenarios: (i) normal hierarchy, where naive power counting holds and two-body currents are suppressed with respect to the LO one-body terms, and (ii) strong hierarchy, where the power counting is distorted and two-body currents dominate. For both scenarios we have observed that in all partial waves the high-energy tail of the response function exhibits log-periodic oscillations. In contrast, at threshold, log-periodic oscillations appear only in the leading $s$-wave multipole. These oscillations are the manifestation of the Efimov effect in photoreactions. Considering photoassociation reactions in ultracold atomic gases, we have concluded that contemporary frozen-spin reactions fall into the category of strong hierarchy. We have found that for temperatures of the order of magnitude of the trimer's binding energy, the oscillations appear to have a pronounced structure that can hopefully be observed experimentally without fine tuning.

*Ackowledgments*. We acknowledge constructive discussions with Chen Ji, Daniel Phillips, Evgeny Epelbaum, and Winfried Leidemann. This work was supported by the Israel Science Foundation (Grant No. 954/09).

[1] E. Braaten and H.-W. Hammer, Phys. Rep. **428**, 259 (2006).
[2] R. E. Grisenti, W. Schöllkopf, J. P. Toennies, G. C. Hegerfeldt, T. Köhler, and M. Stoll, Phys. Rev. Lett. **85**, 2284 (2000).
[3] S. Inouye, M. R. Andrews, J. Stenger, H.-J. Miesner, D. M. Stamper-Kurn, and W. Ketterle, Nature (London) **392**, 151 (1998).
[4] V. Efimov, Phys. Lett. B **33**, 563 (1970).
[5] T. Kraemer, M. Mark, P. Waldburger, J. G. Danzl, C. Chin, B. Engeser, A. D. Lange, K. Pilch, A. Jaakkola, H.-C. Ngerl, and R. Grimm, Nature (London) **440**, 315 (2006).
[6] B. D. Esry, C. H. Greene, and J. P. Burke, Phys. Rev. Lett. **83**, 1751 (1999).
[7] P. F. Bedaque, E. Braaten, and H.-W. Hammer, Phys. Rev. Lett. **85**, 908 (2000).

[8] M. Zaccanti, B. Deissler, C. D'Errico, M. Fattori, M. Jona-Lasinio, S. Muller, G. Roati, M. Inguscio, and G. Modugno, Nat. Phys. **5**, 586 (2009).

[9] S. E. Pollack, D. Dries, and R. G. Hulet, Science **326**, 1683 (2009).

[10] N. Gross, Z. Shotan, S. Kokkelmans, and L. Khaykovich, Phys. Rev. Lett. **103**, 163202 (2009).

[11] N. Gross, Z. Shotan, O. Machtey, S. Kokkelmans, and L. Khaykovich, C. R. Phys. **12**, 4 (2011).

[12] V. Efimov, Yad. Fiz. **29**, 1058 (1979) [Sov. J. Nucl. Phys. **29**, 546 (1979)].

[13] Y. Wang and B. D. Esry, New J. Phys. **13**, 035025 (2011).

[14] D. B. Kaplan, arXiv:nucl-th/0510023.

[15] Y.-H. Song, R. Lazauskas, and T.-S. Park, Phys. Rev. C **79**, 064002 (2009).

[16] E. Braaten, D. Kang, and L. Platter, Phys. Rev. Lett. **106**, 153005 (2011).

[17] T. V. Tscherbul and S. T. Rittenhouse, Phys. Rev. A **84**, 062706 (2011).

[18] B. Bazak, E. Liverts, and N. Barnea, Phys. Rev. A **86**, 043611 (2012).

[19] E. Liverts, B. Bazak, and N. Barnea, Phys. Rev. Lett. **108**, 112501 (2012).

[20] S. Pastore, L. Girlanda, R. Schiavilla, and M. Viviani, Phys. Rev. C **84**, 024001 (2011).

[21] D. Rozpedzik, J. Golak, S. Kölling, E. Epelbaum, R. Skibinski, H. Witała, and H. Krebs, Phys. Rev. C **83**, 064004 (2011).

[22] T. Lompe, T. B. Ottenstein, F. Serwane, A. N. Wenz, G. Zrn, and S. Jochim, Science **330**, 940 (2010).

[23] S. Nakajima, M. Horikoshi, T. Mukaiyama, P. Naidon, and M. Ueda, Phys. Rev. Lett. **106**, 143201 (2011).

[24] O. Machtey, Z. Shotan, N. Gross, and L. Khaykovich, Phys. Rev. Lett. **108**, 210406 (2012).

[25] P. J. Siemens and A. S. Jensen, *Elements of Nuclei: Many-Body Physics with the Strong Interaction* (Addison-Wesley, New York, 1987).

[26] J. Macek, J. Phys. B: At. Mol. Phys. **1**, 831 (1968).

[27] J. Avery, *Hyperspherical Harmonics: Applications in Quantum Theory* (Kluwer Academic, Dordrecht, 1989).

[28] For $q < \kappa$ this approximation amounts to an error $\Delta\mathcal{I}/\mathcal{I} \sim x_n^{m+2}$, where $x_0 \approx 0.06$ is the largest zero of $K_{is_0}(x)$ and $x_n$ is the $n$th root.

[29] B. Bazak and N. Barnea (unpublished).